

Theory of homogeneous linewidths of impurities in polymers and glasses

P. Reineker* and H. Morawitz
 IBM Research Laboratory, San Jose, California 95193

K. Kassner
 University of Ulm, 7900 Ulm, Germany
 (Received 17 October 1983)

A microscopic model for the dephasing of optical impurities in amorphous hosts such as glasses or polymers is presented. The characteristics of the host system are taken into account via two-level systems (TLS's) proposed some time ago to explain the low-temperature properties of inorganic glasses. The TLS's couple to the impurity and to the vibrational degrees of freedom of the matrix. Exact eigenvalues of the equation of motion for correlation functions describing the optical line shape are obtained. In the case of weak coupling between TLS's and impurity, and after averaging over the parameter regime characterizing the TLS's it is found that the optical linewidth depends strongly on the boundaries of this regime. At temperatures well below the Debye temperature one obtains a crossover from a quadratic to a linear temperature increase of the linewidth in the case of coupling to acoustic vibrations, and a crossover from exponential to linear for coupling to optical (librational) modes.

I. INTRODUCTION

In the past several years a considerable number of experimental papers on dephasing in inorganic and organic glasses and polymers have appeared.¹⁻²⁴ This is due to the advent of novel, high-resolution spectroscopic techniques such as fluorescence line narrowing,^{3,5,8,12} photo-physical^{6,7,9,21} and photochemical^{1,2,4,10,11,13-17,19,20} hole burning, and accumulated echoes.²³

Considerable effort has been expended to explain the temperature dependence of the homogeneous linewidths of various impurities. In particular, the exceedingly large range ($6 < T < 300$ K) of the T^2 dependence of Pr^{3+} in BeF_2 and GeO_2 (Ref. 8) has presented a difficult challenge. For some other impurity-amorphous-host combinations, homogeneous widths with a linear temperature dependence^{6,7,9,13} as well as a superlinear T^α dependence ($\alpha=1.3$) (Refs. 19 and 20) have been observed. As the most general feature of homogeneous linewidths of impurities in glasses, we note that at low temperatures they exceed the same parameter in crystalline solids by 1-2 orders of magnitude. In order to account for this very large difference in dephasing time, the existence of low-frequency degrees of freedom is required. Such degrees of freedom have been postulated by Anderson, Halperin, and Varma,²⁵ and by Phillips,²⁶ to explain other anomalous properties of glasses and are discussed in Ref. 27. These degrees of freedom are considered to be a broad distribution of two-level systems (TLS's) describing various degenerate energy states of the glass separated by barriers. In a configuration-coordinate model the two energy levels may be thought of as the two lowest states in a double-well potential with a tunneling barrier separating them (see Fig. 1).

To connect the temperature dependence of the homogeneous linewidth of impurities to the TLS's and vibra-

tions of the host glass, a variety of theoretical models has been proposed.²⁸⁻³⁷ These various models include (1) pseudo-spin-diffusion²⁸ between an isolated impurity and several TLS's, (2) coupling of the ground and the excited state of the impurity to different TLS's,^{29,30} (3) coupling of the ground and excited states of the impurity to TLS's, which communicate by phonon-mediated tunneling,^{31,35} (4) coupling of an impurity to a TLS and direct coupling to a local librational mode,³⁶ and (5) use of fractons instead of phonons as inducing the tunneling of the TLS's.³⁷

These models produce a range of temperature dependences between T and $T^{2.2}$ which depends on various details of the physical mechanisms and TLS parameters used. A satisfactory explanation of the experimental data from a general point of view is not available despite these efforts.

In this paper we present a detailed development of one of the models mentioned above and compare it to other

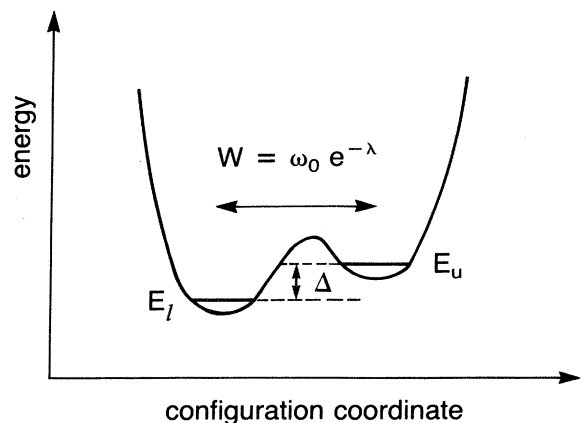


FIG. 1. TLS represented in a configuration-coordinate model by a double-well potential.

treatments. In Sec. II we write the model Hamiltonian, introduce the notation, and transform it to an exactly diagonalized four-level system interacting with vibrations of the matrix. In Sec. III an equation of motion for the reduced density operator ρ of the system is derived, treating the phonons as a heat bath. Section IV derives a set of differential equations for the various dipole correlation functions and finds their exact eigenvalues. In Sec. V we expand the exact eigenvalues found previously and carry out the averages over the parameters characterizing the TLS and its coupling to the impurities and vibrations. Section VI presents a summary of our results and outlook on future work. Appendix A contains a summary of abbreviations used in the main body of the text. Appendix B gives an alternative approach to the derivation of the coupled system of equations for the correlation functions via the density matrix.

II. HAMILTONIAN OF THE MODEL

We wish to calculate the temperature dependence of the optical linewidth of an impurity in a glassy matrix. To that end we introduce the Hamiltonian of the model system, some basic notation, and write the Hamiltonian in a prediagonalized form. We start from the following model whose basic features go back to Lyo and Orbach.³¹ The impurity is described in the simplest possible way by only two energy levels, and it is assumed that the characteristic degrees of freedom of the glass are the so-called TLS's with a broad distribution of low-lying excitation energies; the third component in the model are the vibrational degrees of freedom of the matrix. In the model we assume an interaction between the impurity and a single TLS. The most probable interaction is an electrostatic one and can be thought of in terms of a multipole expansion. The TLS's, in turn, are coupled to the vibrations of the matrix. A direct coupling between the impurity and the vibrations is not taken into account because it is believed that its contribution to the optical linewidth is comparable in both glasses and crystals and therefore negligible at low temperatures. At elevated temperatures corresponding to a $k_B T$ value greater than the relevant phonon energies, the direct coupling between impurities and phonons becomes important. This is obvious from the comparison of the linewidth in crystals and glasses. The Hamiltonian of this model is given by

$$H = H_1 + H_2 + H_3 + H_{12} + H_{23} . \quad (2.1)$$

H_1 is the Hamiltonian of the impurity, $|\alpha\rangle$ and $|\beta\rangle$ are its ground and excited states with energies E_α and E_β , and

$$H_1 = \sum_{\rho=\alpha}^{\beta} E_\rho |\rho\rangle\langle\rho| . \quad (2.2)$$

The Hamiltonian H_2 of the TLS (see Fig. 1) is represented in the following way:

$$H_2 = E_l |l\rangle\langle l| + E_u |u\rangle\langle u| + \frac{W}{2} (|l\rangle\langle u| + |u\rangle\langle l|) . \quad (2.3)$$

E_l and E_u are the energies of the lower and upper states $|l\rangle$ and $|u\rangle$ in the double-well potential, respectively, and $W/2$ is the tunneling matrix element through the potential barrier. The energy asymmetry between the upper and lower states in the double-well potential is

$$\Delta = E_u - E_l . \quad (2.4)$$

The vibrations of the glass matrix are described by the Hamiltonian

$$H_3 = \sum_{qs} \omega_{qs} b_{qs}^\dagger b_{qs} . \quad (2.5)$$

Here ω_{qs} is the energy of a vibration with "wave number" q in branch s . The interaction between the impurity and the TLS is contained in

$$H_{12} = \sum_{\rho=\alpha}^{\beta} (V_{l\rho} |l\rangle\langle l| + V_{u\rho} |u\rangle\langle u|) |\rho\rangle\langle\rho| . \quad (2.6)$$

$V_{l\rho}$ and $V_{u\rho}$ are the coupling matrix elements of the impurity in state $|\rho\rangle$ with the TLS in its lower and upper states, respectively. The coupling matrix elements have to be different in order to enable this interaction to contribute to dephasing. The interaction between the TLS's and the vibrations of the matrix is given by a deformation potential and expressed by the following Hamiltonian:

$$H_{23} = \sum_{qs} \sum_{j=l}^u \frac{1}{\sqrt{N}} h_{qs}^j (b_q + b_{-q}^\dagger) |j\rangle\langle j| . \quad (2.7)$$

The coupling matrix elements h_{qs}^j , $j=l, u$, are proportional to the deformation potential and also need to be different for the lower and upper states. In Sec. III we will treat the phonons as a reservoir interacting via H_{23} with the system consisting of an impurity and a TLS. In this way we arrive at the following grouping of the terms in the Hamiltonian:

$$H = H_S + H_R + H_{SR} , \quad (2.8)$$

$$H_S = H_1 + H_2 + H_{12} , \quad (2.9)$$

$$H_R = H_3 , \quad (2.10)$$

$$H_{SR} = H_{23} , \quad (2.11)$$

where H_S and H_R are the system and reservoir Hamiltonians, respectively, and H_{SR} describes the interaction between them.

A. Diagonalization of the TLS Hamiltonian H_2

The Hamiltonian of the TLS, H_2 , is given by (2.3) and can be diagonalized exactly. The wave functions in the Schrödinger equation,

$$H_2 |\psi_i\rangle = E_i |\psi_i\rangle , \quad (2.12)$$

are written as a superposition of the lower and upper states, $|l\rangle$ and $|u\rangle$, respectively, in the double-well potential, in the following form:

$$|\psi_i\rangle = C_{1i} |l\rangle + C_{2i} |u\rangle , \quad i = 1, 2 . \quad (2.13)$$

Explicitly, the eigenvalues are given by

$$E_{1,2} = \frac{1}{2}(E_u + E_l \mp E), \quad (2.14)$$

$$C_{11} = C_{22} = \sin\phi, \quad C_{21} = -C_{12} = -\cos\phi, \quad (2.15)$$

with

$$\tan\phi = \left[\frac{E + \Delta}{E - \Delta} \right]^{1/2} \quad (2.16)$$

and

$$E = (\Delta^2 + W^2)^{1/2}. \quad (2.17)$$

The diagonalized form of the Hamiltonian then reads

$$H_2 = \sum_{i=1}^2 E_i |\psi_i\rangle \langle \psi_i|. \quad (2.18)$$

In the following we need the transformation between the eigenstates $|\psi_1\rangle, |\psi_2\rangle$ and basis vectors $|l\rangle, |u\rangle$, which is written concisely as

$$\begin{bmatrix} |\psi_1\rangle \\ |\psi_2\rangle \end{bmatrix} = \begin{bmatrix} \sin\phi & -\cos\phi \\ \cos\phi & \sin\phi \end{bmatrix} \begin{bmatrix} |l\rangle \\ |u\rangle \end{bmatrix}, \quad (2.19a)$$

$$\begin{bmatrix} |l\rangle \\ |u\rangle \end{bmatrix} = \begin{bmatrix} \sin\phi & \cos\phi \\ -\cos\phi & \sin\phi \end{bmatrix} \begin{bmatrix} |\psi_1\rangle \\ |\psi_2\rangle \end{bmatrix}. \quad (2.19b)$$

B. Diagonalization of the system Hamiltonian H_S

Equation (2.9) gives the system Hamiltonian H_S . With the use of the transformation (2.19) the Hamiltonian H_{12} describes the interaction between the impurity and a TLS becomes

$$H_{12} = \sum_{\rho=\alpha}^{\beta} \left[S_{\rho} + V_{\rho} \frac{\Delta}{E} (|\psi_1\rangle \langle \psi_1| - |\psi_2\rangle \langle \psi_2|) + V_{\rho} \frac{W}{E} (|\psi_1\rangle \langle \psi_2| + |\psi_2\rangle \langle \psi_1|) \right] |\rho\rangle \langle \rho|, \quad (2.20)$$

with

$$S_{\rho} = \frac{1}{2}(V_{l\rho} + V_{u\rho}) \quad (2.21)$$

and

$$V_{\rho} = \frac{1}{2}(V_{l\rho} - V_{u\rho}). \quad (2.22)$$

The eigenstates of the Schrödinger equation,

$$H_S |i\rangle = \epsilon_i |i\rangle, \quad (2.23)$$

are expressed in terms of product states $|\psi_{i,\rho}\rangle = |\psi_i\rangle |\rho\rangle$ ($\rho = \alpha, \beta$) in the following form:

$$|i\rangle = C_{1i} |\psi_1, \alpha\rangle + C_{2i} |\psi_1, \beta\rangle + C_{3i} |\psi_2, \alpha\rangle + C_{4i} |\psi_2, \beta\rangle, \quad i = 1, \dots, 4. \quad (2.24)$$

The four eigensolutions are given by

$$\epsilon_1 = E_{\alpha} + S_{\alpha} + \frac{E_1 + E_2}{2} - [(E/2)^2 - V_{\alpha}\Delta + V_{\alpha}^2]^{1/2} = \epsilon_1^{\alpha}, \quad (2.25a)$$

$$C_{11} = \sin\alpha, \quad C_{31} = -\cos\alpha, \quad C_{21} = C_{41} = 0, \quad (2.25b)$$

$$\epsilon_2 = E_{\alpha} + S_{\alpha} + \frac{E_1 + E_2}{2} + [(E/2)^2 - V_{\alpha}\Delta + V_{\alpha}^2]^{1/2} = \epsilon_2^{\alpha}, \quad (2.26a)$$

$$C_{12} = \cos\alpha, \quad C_{32} = \sin\alpha, \quad C_{22} = C_{42} = 0, \quad (2.26b)$$

$$\epsilon_3 = E_{\beta} + S_{\beta} + \frac{E_1 + E_2}{2} - [(E/2)^2 - V_{\beta}\Delta + V_{\beta}^2]^{1/2} = \epsilon_1^{\beta}, \quad (2.27a)$$

$$C_{13} = C_{33} = 0, \quad C_{23} = \sin\beta, \quad C_{43} = -\cos\beta, \quad (2.27b)$$

$$\epsilon_4 = E_{\beta} + S_{\beta} + \frac{E_1 + E_2}{2} + [(E/2)^2 - V_{\beta}\Delta + V_{\beta}^2]^{1/2} = \epsilon_2^{\beta}, \quad (2.28a)$$

$$C_{14} = C_{34} = 0, \quad C_{24} = \cos\beta, \quad C_{44} = \sin\beta. \quad (2.28b)$$

$\cos\alpha$ and $\sin\alpha$ are given by

$$\left. \begin{array}{l} \cos\alpha \\ \sin\alpha \end{array} \right\} = \frac{1}{\sqrt{2}} \left[1 \mp \frac{E - 2V_{\alpha}(\Delta/E)}{(E^2 - 4V_{\alpha}\Delta + 4V_{\alpha}^2)^{1/2}} \right]^{1/2}, \quad (2.29)$$

and $\cos\beta$ and $\sin\beta$ are obtained by replacing V_{α} and V_{β} on the right-hand side.

The diagonalized form of the Hamiltonian becomes

$$H_S = \sum_{i=1}^4 \epsilon_i |i\rangle \langle i|. \quad (2.30)$$

The eigenvalue spectrum consists of two closely spaced pairs of energy levels (see Fig. 2) when the energy splitting E in the TLS and the interaction V_{ρ} between the TLS and the impurity are small compared to the energy difference between the ground and the excited state of the impurity.

The transformation between the eigenstates $|1\rangle, |2\rangle$ and the basis vectors $|\psi_{1,\alpha}\rangle, |\psi_{2,\alpha}\rangle$ is given by

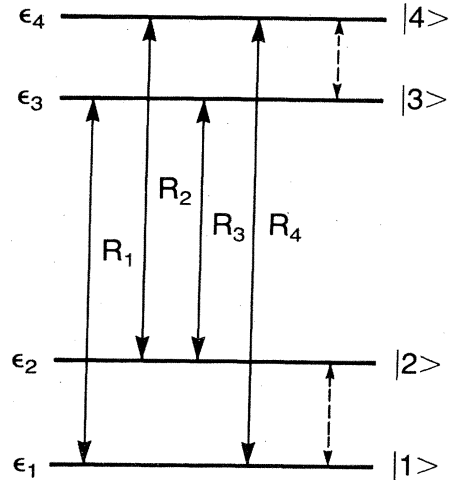


FIG. 2. Energy-level scheme of the system Hamiltonian H_S . The solid-line arrows indicate optical transitions, and the dashed-line ones show phonon-induced relaxation.

$$\begin{pmatrix} |1\rangle \\ |2\rangle \end{pmatrix} = \begin{pmatrix} \sin\alpha & -\cos\alpha \\ \cos\alpha & \sin\alpha \end{pmatrix} \begin{pmatrix} |\psi_1, \alpha\rangle \\ |\psi_2, \alpha\rangle \end{pmatrix}, \quad (2.31a)$$

$$\begin{pmatrix} |\psi_1, \alpha\rangle \\ |\psi_2, \alpha\rangle \end{pmatrix} = \begin{pmatrix} \sin\alpha & \cos\alpha \\ -\cos\alpha & \sin\alpha \end{pmatrix} \begin{pmatrix} |1\rangle \\ |2\rangle \end{pmatrix}. \quad (2.31b)$$

The transformation for the eigenstates $|3\rangle$ and $|4\rangle$ is obtained from (2.31) by the following replacements:

$$|1\rangle \rightarrow |3\rangle, \quad |2\rangle \rightarrow |4\rangle, \quad (2.32a)$$

$$|\psi_i, \alpha\rangle \rightarrow |\psi_i, \beta\rangle, \quad \alpha \rightarrow \beta. \quad (2.32b)$$

C. Interaction between TLS and matrix vibrations

The Hamiltonian describing the interaction between the TLS and the vibrations of the matrix is given by (2.11) and (2.7). With the use of the transformation (2.19), H_{SR} becomes

$$\begin{aligned} H_{SR} &= H_{23} \\ &= \sum_{qs} \left[S_{qs} + \frac{\Delta}{E} D_{qs} (|\psi_1\rangle\langle\psi_1| - |\psi_2\rangle\langle\psi_2|) \right. \\ &\quad \left. + \frac{W}{E} D_{qs} (|\psi_1\rangle\langle\psi_2| \right. \\ &\quad \left. + |\psi_2\rangle\langle\psi_1|) \right] (b_q + b_{-q}^\dagger), \quad (2.33) \end{aligned}$$

with

$$S_{qs} = \frac{h_{qs}^l + h_{qs}^u}{2\sqrt{N}}, \quad (2.34)$$

$$D_{qs} = \frac{h_{qs}^l - h_{qs}^u}{2\sqrt{N}}. \quad (2.35)$$

Lyo and Orbach³¹ took into account only the last (off-diagonal) term of (2.33). In a later paper, Lyo^{34,35} also included the diagonal part, and argued it would dominate the dephasing. In our exact diagonalization (2.36) of the full four-level system we included both terms throughout. The differentiation between distinct diagonal and nondiagonal interactions³⁴ can be misleading in different parameter ranges of the TLS because of partial compensation between these terms. Lyo seems to have recently noticed this fact.³⁵

With the use of the transformations (2.31) and (2.32) to the eigenstates of H_S , H_{SR} is written in the following form:

$$H_{SR} = \sum_{qs} \Omega_{qs} \epsilon_{qs}. \quad (2.36)$$

In this expression we have used the following abbreviations:

$$\begin{aligned} \Omega_{qs} &= \Pi_{qs} + D_{qs} \{ B_\alpha (|1\rangle\langle 2| + |2\rangle\langle 1|) \\ &\quad + B_\beta (|3\rangle\langle 4| + |4\rangle\langle 3|) \}, \quad (2.37) \end{aligned}$$

$$\begin{aligned} \Pi_{qs} &= S_{qs} + D_{qs} \{ A_\alpha (|2\rangle\langle 2| - |1\rangle\langle 1|) \\ &\quad + A_\beta (|4\rangle\langle 4| - |3\rangle\langle 3|) \}, \quad (2.38) \end{aligned}$$

$$\begin{aligned} A_\alpha &= (\Delta/E)(\cos^2\alpha - \sin^2\alpha) + 2(W/E)\sin\alpha \cos\alpha \\ &= (\Delta/E)\cos 2\alpha + (W/E)\sin 2\alpha, \quad (2.39) \end{aligned}$$

$$\begin{aligned} B_\alpha &= 2(\Delta/E)\sin\alpha \cos\alpha - (W/E)(\cos^2\alpha - \sin^2\alpha) \\ &= (\Delta/E)\sin 2\alpha - (W/E)\cos 2\alpha, \quad (2.40) \end{aligned}$$

$$\epsilon_{qs} = b_{qs} + b_{-qs}^\dagger. \quad (2.41)$$

In Fig. 2 we have indicated by solid-line arrows the four possible optical transitions R_1, \dots, R_4 . The dashed-line arrows indicate relaxation transitions which are introduced by the interaction with vibrations and which are contained in Eqs. (2.36) and (2.37). This simple picture allows some qualitative discussion of the behavior of the optical spectra. Generally, the optical line will be composed of four contributions corresponding to R_1, \dots, R_4 . The lifetimes of levels 1 and 3, connected by the transition R_1 , are shortened by phonon-induced transitions to levels 2 and 4 under phonon absorption. With increasing temperature, we have an increasing transition rate and therefore a broadening of the line. For very low temperatures, however, phonon absorption is no longer possible and therefore this contribution to the optical line becomes very narrow. The optical transition R_2 connects levels 2 and 4, which may decay to levels 1 and 3 on account of phonon emission. At very low temperatures spontaneous phonon emission is still possible, and therefore this contribution to the optical line remains finite even at $T=0$ K. Similar arguments apply to the transitions R_3 and R_4 where phonon-absorption and -emission processes are involved. Another interesting feature may be seen from Fig. 2. The frequencies of optical transitions R_1 and R_2 are very close to each other. For small phonon-induced scattering rates, compared to the difference in optical frequencies, we have a broadening of the contributions from R_1 and R_2 to the optical line. For large scattering rates, however, we expect a motional narrowing in this contribution. The line shape actually observed will finally also depend on the size of the transition dipole moments and on the occupation probabilities of the various levels.

III. DENSITY OPERATOR OF THE SYSTEM

In this section we derive the equation of motion for the density operator of the system. As stated earlier the system consists of the impurity and the TLS along with their interactions. The phonons are treated as a heat bath coupled weakly to the system. The density-operator equation allows one to discuss the time development of the system, and we shall use it in Sec. IV to derive equations of motion for two-time correlation functions relevant to optical line shapes. The equation of motion for the density operator of the coupled system and bath is

$$\dot{W}(t) = -i[H, W(t)], \quad (3.1)$$

with the Hamiltonian H given by (2.8). $W(t)$ is the total density operator of the system and the reservoir. The re-

duced density operator of the system, $\rho(t)$, is obtained by taking the trace over the variables of the reservoir,

$$\rho(t) = \text{Tr}_R W(t). \quad (3.2)$$

The equation of motion for this quantity is obtained from (3.1) using the Nakajima-Zwanzig projection technique.^{38,39} Introducing the Born and Markov approximations,^{40,41} we arrive at

$$\begin{aligned} \frac{d}{dt}\rho(t) = & -i[H_S, \rho(t)] - \sum_{qs} \sum_{q's'} \int_0^\infty d\tau \{ \text{Tr}_R [\epsilon_{qs} \epsilon_{q's'}(-\tau) \rho_0] [\Omega_{qs} \Omega_{q's'}(-\tau) \rho(t) - \Omega_{q's'}(-\tau) \rho(t) \Omega_{qs}] \\ & + \text{Tr}_R [\epsilon_{q's'}(-\tau) \epsilon_{qs} \rho_0] [\rho(t) \Omega_{q's'}(-\tau) \Omega_{qs} - \Omega_{qs} \rho(t) \Omega_{q's'}(-\tau)] \}. \end{aligned} \quad (3.3)$$

The interaction representation of the operators Ω_{qs} and ϵ_{qs} which are defined in (2.37) and (2.41) are given by

$$\Omega_{qs}(-\tau) = e^{-iH_S\tau} \Omega_{qs} e^{iH_S\tau}, \quad (3.4)$$

$$\epsilon_{qs}(-\tau) = e^{-iH_R\tau} \epsilon_{qs} e^{iH_R\tau}. \quad (3.5)$$

ρ_0 is the equilibrium density operator of the reservoir, and is given by

$$\rho_0 = \frac{e^{-\beta H_R}}{\text{Tr}_R e^{-\beta H_R}}. \quad (3.6)$$

The evaluation of the integrals may easily be carried out, and introducing the abbreviations

$$P_{ij}^{qs}(r) = P \frac{1}{\omega_{qs} - \epsilon_i + \epsilon_j} (n_{qs} + r) \quad (3.7)$$

and

$$\delta_{ij}^{qs}(r) = \pi \delta(\omega_{qs} - \epsilon_i + \epsilon_j) (n_{qs} + r), \quad r = 0, 1 \quad (3.8)$$

the equation of motion for the density operator becomes

$$\begin{aligned} \dot{\rho}(t) = & -i[H_S, \rho(t)] + i \sum_{qs} P \frac{1}{\omega_{qs}} [\Omega_{qs}, \Pi_{-qs} \rho(t) + \rho(t) \Pi_{-qs}] + i \sum_{qs} [P_{21}^{qs}(1) - P_{12}^{qs}(0)] D_{-qs} B_\alpha K_{12}^\dagger \\ & + i \sum_{qs} [-P_{21}^{qs}(0) + P_{12}^{qs}(1)] D_{-qs} B_\alpha K_{21}^\dagger + i \sum_{qs} [P_{43}^{qs}(1) - P_{34}^{qs}(0)] D_{-qs} B_\beta K_{34}^\dagger + i \sum_{qs} [-P_{43}^{qs}(0) + P_{34}^{qs}(1)] D_{-qs} B_\beta K_{43}^\dagger \\ & - \sum_{qs} \pi \delta(\omega_{qs}) (2n_{qs} + 1) [\Omega_{qs}, \Pi_{-qs} \rho(t) - \rho(t) \Pi_{-qs}] - \sum_{qs} [\delta_{21}^{qs}(1) + \delta_{12}^{qs}(0)] D_{-qs} B_\alpha K_{12}^- \\ & - \sum_{qs} [\delta_{21}^{qs}(0) + \delta_{12}^{qs}(1)] D_{-qs} B_\alpha K_{21}^- - \sum_{qs} [\delta_{43}(1) + \delta_{34}(0)] D_{-qs} B_\beta K_{34}^- - \sum_{qs} [\delta_{43}(0) + \delta_{34}(1)] D_{-qs} B_\beta K_{43}^-, \end{aligned} \quad (3.9a)$$

$$K_{ij}^\pm = [\Omega_{qs}, |i\rangle \langle j| \rho(t) \pm \rho(t) |j\rangle \langle i|]. \quad (3.9b)$$

In writing this equation we have used Π_{qs} from (2.38), and B_β from (2.40).

Explicitly, the equation of motion for the density-matrix elements, using the eigenstates (2.24) as basis vectors, reads

$$\dot{\rho}_{11} = -W_{12}\rho_{11} + W_{21}\rho_{22} - 2(iP_0 + \Delta_0 A_\alpha) B_\alpha \rho_{12} + 2(iP_0 - \Delta_0 A_\alpha) B_\alpha \rho_{21}, \quad (3.10)$$

$$\dot{\rho}_{22} = -\dot{\rho}_{11}, \quad (3.11)$$

$$\begin{aligned} \dot{\rho}_{12} = & 2(-i\{P_0 - A_\alpha[P_1 + P_2(0)]\} - \Delta_2(0)A_\alpha) B_\alpha \rho_{11} + 2(i\{P_0 + A_\alpha[P_1 - P_2(1)]\} + \Delta_2(1)A_\alpha) B_\alpha \rho_{22} \\ & + \{-i(\tilde{\epsilon}_1 - \tilde{\epsilon}_2) - \frac{1}{2}(W_{12} + W_{21}) - 4\Delta_0 A_\alpha^2\} \rho_{12} + \{-i[P_2(0) + P_2(1)] B_\alpha^2 + \frac{1}{2}(W_{12} + W_{21})\} \rho_{21}, \end{aligned} \quad (3.12)$$

$$\rho_{21} = \rho_{12}^*, \quad (3.13)$$

$$\begin{aligned} \dot{\rho}_{31} = & [-i(\tilde{\epsilon}_3 - \tilde{\epsilon}_1) - \frac{1}{2}(W_{12} + W_{34}) - \Delta_0(A_\alpha - A_\beta)^2] \rho_{31} + \{i[P_2(1) - P_4(1)] + \Delta_2(1) + \Delta_4(1)\} B_\alpha B_\beta \rho_{42} \\ & + (-i\{2P_0 + (A_\alpha - A_\beta)[P_1 - P_2(1)]\} + \Delta_2(1)(A_\alpha - A_\beta) - \Delta_0(A_\alpha + A_\beta)) B_\alpha \rho_{32} \\ & + (i\{2P_0 - (A_\alpha - A_\beta)[P_1 - P_4(1)] - \Delta_4(1)(A_\alpha - A_\beta) - \Delta_0(A_\alpha + A_\beta)\} B_\beta \rho_{41}, \end{aligned} \quad (3.14)$$

$$\begin{aligned} \dot{\rho}_{42} = & \{-i[P_2(0) - P_4(0)] + \Delta_2(0) + \Delta_4(0)\} B_\alpha B_\beta \rho_{31} + [-i(\tilde{\epsilon}_4 - \tilde{\epsilon}_2) - \frac{1}{2}(W_{21} + W_{43}) - \Delta_0(A_\alpha - A_\beta)^2] \rho_{42} \\ & + (i\{2P_0 + (A_\alpha - A_\beta)[P_1 + P_4(0)]\} + \Delta_4(0)(A_\alpha - A_\beta) + \Delta_0(A_\alpha + A_\beta)) B_\beta \rho_{32} \\ & + (-i\{2P_0 - (A_\alpha - A_\beta)[P_1 + P_2(0)]\} - \Delta_2(0)(A_\alpha - A_\beta) + \Delta_0(A_\alpha + A_\beta)) B_\alpha \rho_{41}, \end{aligned} \quad (3.15)$$

$$\begin{aligned} \dot{\rho}_{32} = & (-i\{2P_0 - (A_\alpha + A_\beta)[P_1 + P_2(0)]\} - \Delta_2(0)(A_\alpha + A_\beta) + \Delta_0(A_\alpha - A_\beta)) B_\alpha \rho_{31} \\ & + (i\{2P_0 + (A_\alpha + A_\beta)[P_1 - P_4(1)]\} + \Delta_4(1)(A_\alpha + A_\beta) + \Delta_0(A_\alpha - A_\beta)) B_\beta \rho_{42} \\ & + [-i(\tilde{\epsilon}_3 - \tilde{\epsilon}_2) - \frac{1}{2}(W_{21} + W_{34}) - \Delta_0(A_\alpha + A_\beta)^2] \rho_{32} + \{-i[P_2(0) + P_4(1)] + \Delta_2(0) + \Delta_4(1)\} B_\alpha B_\beta \rho_{41}, \end{aligned} \quad (3.16)$$

$$\begin{aligned} \dot{\rho}_{41} = & (i\{2P_0 - (A_\alpha + A_\beta)[P_1 + P_4(0)]\} - \Delta_4(0)(A_\alpha + A_\beta) - \Delta_0(A_\alpha - A_\beta)) B_\beta \rho_{31} \\ & + (-i\{2P_0 + (A_\alpha + A_\beta)[P_1 - P_2(1)]\} + \Delta_2(1)(A_\alpha + A_\beta) - \Delta_0(A_\alpha - A_\beta)) B_\alpha \rho_{42} \\ & + \{i[P_2(1) + P_4(0)] + \Delta_2(1) + \Delta_4(0)\} B_\alpha B_\beta \rho_{32} + [-i(\tilde{\epsilon}_4 - \tilde{\epsilon}_1) - \frac{1}{2}(W_{12} + W_{43}) - \Delta_0(A_\alpha + A_\beta)^2] \rho_{41}. \end{aligned} \quad (3.17)$$

The factors P_i and $P_j(r)$ contain the principal-value parts, and the quantities Δ_0 and $\Delta_j(r)$, contain the δ -function parts of integrals of the form $\int_0^\infty \exp(i\omega t) dt$. Explicitly, these quantities are defined in (A1)–(A11). Equations (3.10) and (3.11) for the occupation numbers of levels 1 and 2 (see Fig. 2) show that vibrations induce transitions only between these two levels, and that there is no coupling to the occupation numbers of levels 3 and 4. The transition rates between the levels are W_{12} and W_{21} and defined in (A12) and (A13). In addition to these transitions, there is also a coupling of the off-diagonal elements ρ_{12} and ρ_{21} . Analogously, the time derivatives of these quantities couple to the occupation numbers ρ_{11} and ρ_{22} , and to ρ_{12} and ρ_{21} . In these equations, the quantity $\tilde{\epsilon}_1 - \tilde{\epsilon}_2$ occurs, which is the difference of renormalized energies in (A16) and (A17). The equations for ρ_{33} , ρ_{44} , ρ_{34} , and ρ_{43} are obtained from (3.10)–(3.13) by replacing $1 \rightarrow 3$ and $2 \rightarrow 4$ with $P_3 = P_1$; they also form a closed set. Inspection of (3.14)–(3.17) shows that the off-diagonal matrix elements ρ_{31} , ρ_{42} , ρ_{32} , and ρ_{41} form a closed set of equations in the same way as their conjugate-complex matrix elements. In the following and in connection with Appendix B we shall see that these are the essential matrix elements for the description of optical absorption.

IV. CORRELATION FUNCTIONS FOR THE OPTICAL LINE SHAPE

To describe the interaction of light with our system we have to couple the light field to the electronic-transition dipole of the impurity. From linear-response theory the optical line shape is determined by the one-sided Fourier transform of the two-time dipole-dipole correlation function as follows:

$$\chi''(\omega) = i \int_0^\infty d\tau \sin \omega \tau \text{Tr}\{P(\tau)[P, \rho_{SO}]\}, \quad (4.1)$$

The dipole operator may be represented by

$$P = \sum_{i=1}^2 \mu (|\psi_i, \alpha\rangle \langle \psi_i, \beta| + |\psi_i, \beta\rangle \langle \psi_i, \alpha|), \quad (4.2)$$

using as basis functions the product states of both the impurity and the TLS, as in (2.24). The transformation (2.31b) to the eigenfunctions of H_S results in

$$P = \mu_1 (|3\rangle \langle 1| + |1\rangle \langle 3| + |4\rangle \langle 2| + |2\rangle \langle 4|) + \mu_2 (|4\rangle \langle 1| + |1\rangle \langle 4| - |3\rangle \langle 2| - |2\rangle \langle 3|), \quad (4.3)$$

with

$$\mu_1 = \mu \cos(\alpha - \beta), \quad (4.4a)$$

$$\mu_2 = \mu \sin(\alpha - \beta), \quad (4.4b)$$

where α and β have been defined in connection with (2.29). On account of the coupling between the impurity and the TLS, the original transition dipole between levels α and β is now replaced by the four transitions indicated by Fig. 2. The reduced density operator ρ_{SO} at the initial time in these states may be represented as

$$\rho_{SO} = \sum_{i=1}^4 \rho_i |i\rangle \langle i|. \quad (4.5)$$

With this representation for ρ_{SO} , we have

$$\begin{aligned} [P, \rho_{SO}] = & \mu_1 [(\rho_1 - \rho_3)(|3\rangle \langle 1| - |1\rangle \langle 3|) + (\rho_2 - \rho_4)(|4\rangle \langle 2| - |2\rangle \langle 4|)] \\ & + \mu_2 [-(\rho_2 - \rho_3)(|3\rangle \langle 2| - |2\rangle \langle 3|) + (\rho_1 - \rho_4)(|4\rangle \langle 1| - |1\rangle \langle 4|)], \end{aligned} \quad (4.6)$$

and the two-time correlation function of the dipole operator reads

$$\begin{aligned} \text{Tr}\{P(\tau)[P, \rho_{SO}]\} = & \mu_1(\rho_1 - \rho_3)[S_1(\tau) - S_1^*(\tau)] + \mu_1(\rho_2 - \rho_4)[S_2(\tau) - S_2^*(\tau)] \\ & - \mu_2(\rho_2 - \rho_3)[S_3(\tau) - S_3^*(\tau)] + \mu_2(\rho_1 - \rho_4)[S_4(\tau) - S_4^*(\tau)], \end{aligned} \quad (4.7)$$

with the following abbreviations for the various two-time correlation functions:

$$S_1(\tau) = \text{Tr}\{P(\tau) | 3 \rangle \langle 1 | \} = \text{Tr}\{P e^{-iL\tau} | 3 \rangle \langle 1 | \} = (P^+, e^{-iL\tau} | 3 \rangle \langle 1 |), \quad (4.8a)$$

$$S_2(\tau) = \text{Tr}\{P(\tau) | 4 \rangle \langle 2 | \} = \text{Tr}\{P e^{-iL\tau} | 4 \rangle \langle 2 | \} = (P^+, e^{-iL\tau} | 4 \rangle \langle 2 |), \quad (4.8b)$$

$$S_3(\tau) = \text{Tr}\{P(\tau) | 3 \rangle \langle 2 | \} = \text{Tr}\{P e^{-iL\tau} | 3 \rangle \langle 2 | \} = (P^+, e^{-iL\tau} | 3 \rangle \langle 2 |), \quad (4.8c)$$

$$S_4(\tau) = \text{Tr}\{P(\tau) | 4 \rangle \langle 1 | \} = \text{Tr}\{P e^{-iL\tau} | 4 \rangle \langle 1 | \} = (P^+, e^{-iL\tau} | 4 \rangle \langle 1 |). \quad (4.8d)$$

In writing (4.8) the quantum regression theorem^{42,43} has been used, and L is the Liouville operator describing the time development of the reduced density operator according to (3.9),

$$\dot{\rho} = -iL\rho. \quad (4.9)$$

A. Equations of motion for the correlation functions

To derive equations of motion for the correlation functions we differentiate $S_1(\tau)$ with respect to τ and arrive at

$$\dot{S}_1(\tau) = (P^+, e^{-iL\tau}(-iL) | 3 \rangle \langle 1 |). \quad (4.10)$$

Applying the Liouville operator L from (3.9) and (4.9), and proceeding in the same way with the other correlation functions of (4.8), we obtain the following closed set of equations for $S_i(\tau)$, $i = 1, \dots, 4$:

$$\begin{aligned} \dot{S}_1(\tau) = & [-i(\tilde{\epsilon}_3 - \tilde{\epsilon}_1) - \frac{1}{2}(W_{12} + W_{34}) - \Delta_0(A_\alpha - A_\beta)^2]S_1 + \{-i[P_2(0) - P_4(0)] + \Delta_2(0) + \Delta_4(0)\}B_\alpha B_\alpha S_2 \\ & + (-i\{2P_0 - [P_1 + P_2(0)](A_\alpha + A_\beta)\} - \Delta_2(0)(A_\alpha + A_\beta) + \Delta_0(A_\alpha - A_\beta))B_\alpha S_3 \\ & + (i\{2P_0 - [P_1 + P_4(0)](A_\alpha + A_\beta)\} - \Delta_4(0)(A_\alpha + A_\beta) - \Delta_0(A_\alpha - A_\beta))B_\beta S_4, \end{aligned} \quad (4.11)$$

$$\begin{aligned} \dot{S}_2 = & \{i[P_2(1) - P_4(1)] + \Delta_2(1) + \Delta_4(1)\}B_\alpha B_\beta S_1 + [-i(\tilde{\epsilon}_4 - \tilde{\epsilon}_2) - \frac{1}{2}(W_{21} + W_{43}) - \Delta_0(A_\alpha - A_\beta)^2]S_2 \\ & + (i\{2P_0 + [P_1 - P_4(1)](A_\alpha + A_\beta) + \Delta_4(1)(A_\alpha + A_\beta)\} + \Delta_0(A_\alpha - A_\beta))B_\beta S_3 \\ & + (-i\{2P_0 + [P_1 - P_2(1)](A_\alpha + A_\beta) + \Delta_2(1)(A_\alpha + A_\beta)\} - \Delta_0(A_\alpha - A_\beta))B_\alpha S_4, \end{aligned} \quad (4.12)$$

$$\begin{aligned} \dot{S}_3 = & (-i\{2P_0 + [P_1 - P_2(1)](A_\alpha - A_\beta)\} + \Delta_2(1)(A_\alpha - A_\beta) - \Delta_0(A_\alpha + A_\beta))B_\alpha S_1 \\ & + (i\{2P_0 + [P_1 + P_4(0)](A_\alpha - A_\beta)\} + \Delta_4(0)(A_\alpha - A_\beta) + \Delta_0(A_\alpha + A_\beta))B_\beta S_2 \\ & + [-i(\tilde{\epsilon}_3 - \tilde{\epsilon}_2) - \frac{1}{2}(W_{21} + W_{34}) - \Delta_0(A_\alpha + A_\beta)^2]S_3 + \{i(P_2(1) + P_4(0)) + \Delta_2(1) + \Delta_4(0)\}B_\alpha B_\beta S_4, \end{aligned} \quad (4.13)$$

$$\begin{aligned} \dot{S}_4 = & (i\{2P_0 - [P_1 - P_4(1)](A_\alpha - A_\beta)\} - \Delta_4(1)(A_\alpha - A_\beta) - \Delta_0(A_\alpha + A_\beta))B_\beta S_1 \\ & + (-i\{2P_0 - [P_1 + P_2(0)](A_\alpha - A_\beta)\} - \Delta_2(0)(A_\alpha - A_\beta) + \Delta_0(A_\alpha + A_\beta))B_\alpha S_2 \\ & + \{-i[P_2(0) + P_4(1)] + \Delta_2(0) + \Delta_4(1)\}B_\alpha B_\beta S_3 + [-i(\tilde{\epsilon}_4 - \tilde{\epsilon}_1) - \frac{1}{2}(W_{12} + W_{43}) - \Delta_0(A_\alpha + A_\beta)^2]S_4. \end{aligned} \quad (4.14)$$

This set of equations may also immediately be obtained from the equations of motion (3.14)–(3.17) for the density matrix, as shown in Appendix B. To simplify the set of equations we shall neglect all principal-value parts in the coefficients of (4.11)–(4.14), and we arrive at the following set of equations for the correlation functions:

$$\dot{S}_1 = [-i(\epsilon_3 - \epsilon_1) - \frac{1}{2}(W_{12} + W_{34})]S_1 + [\Delta_2(0) + \Delta_4(0)]B_\alpha B_\beta S_2 - \Delta_2(0)(A_\alpha + A_\beta)B_\alpha S_3 - \Delta_4(0)(A_\alpha + A_\beta)B_\beta S_4, \quad (4.15)$$

$$\dot{S}_2 = [\Delta_2(1) + \Delta_4(1)]B_\alpha B_\beta S_1 + [-i(\epsilon_4 - \epsilon_2) - \frac{1}{2}(W_{21} + W_{43})]S_2 + \Delta_4(1)(A_\alpha + A_\beta)B_\beta S_3 + \Delta_2(1)(A_\alpha + A_\beta)B_\alpha S_4, \quad (4.16)$$

$$\dot{S}_3 = \Delta_2(1)(A_\alpha - A_\beta)B_\alpha S_1 + \Delta_4(0)(A_\alpha - A_\beta)B_\beta S_2 + [-i(\epsilon_3 - \epsilon_2) - \frac{1}{2}(W_{21} + W_{34})]S_3 + [\Delta_2(1) + \Delta_4(0)]B_\alpha B_\beta S_4, \quad (4.17)$$

$$\dot{S}_4 = -\Delta_4(1)(A_\alpha - A_\beta)B_\beta S_1 - \Delta_2(0)(A_\alpha - A_\beta)B_\alpha S_2 + [\Delta_2(0) + \Delta_4(1)]B_\alpha B_\beta S_3 + [-i(\epsilon_4 - \epsilon_1) - \frac{1}{2}(W_{12} + W_{43})]S_4. \quad (4.18)$$

B. Exact calculation of the eigenvalues

In this subsection we obtain the exact eigenvalues of the simplified set of Eqs. (4.15)–(4.18). With the ansatz

$$S_i(t) = e^{Rt} S_i, \quad (4.19)$$

the solution of the coupled set of differential equations is transformed to a four-dimensional non-Hermitian eigenvalue problem. The exact eigenvalues are given by

$$R_{1,2} = -\frac{1}{2}[A \mp (B + 2\sqrt{C})^{1/2}], \quad (4.20)$$

$$R_{3,4} = -\frac{1}{2}[A \mp (B - 2\sqrt{C})^{1/2}]. \quad (4.21)$$

A , B , and C are abbreviations for the following expressions:

$$A = i(\epsilon_3 - \epsilon_1 + \epsilon_4 - \epsilon_2) + [\Delta_2(1) + \Delta_2(0)]B_\alpha^2 + [\Delta_4(1) + \Delta_4(0)]B_\beta^2, \quad (4.22)$$

$$B = \{i(\epsilon_4 - \epsilon_3) + [\Delta_4(1) - \Delta_4(0)]B_\beta^2\}^2 + \{i(\epsilon_2 - \epsilon_1) - [\Delta_2(1) - \Delta_2(0)]B_\alpha^2\}^2 \\ + 2[\Delta_2(1)B_\alpha^2 + \Delta_4(1)B_\beta^2][\Delta_2(0)B_\alpha^2 + \Delta_4(0)B_\beta^2] + 2[\Delta_2(1)B_\alpha^2 + \Delta_4(0)B_\beta^2][\Delta_2(0)B_\alpha^2 + \Delta_4(1)B_\beta^2], \quad (4.23)$$

$$C = \{-(\epsilon_4 - \epsilon_3)(\epsilon_2 - \epsilon_1) + i(\epsilon_2 - \epsilon_1)[\Delta_4(1) - \Delta_4(0)]B_\beta^2 - i(\epsilon_4 - \epsilon_3)[\Delta_2(1) - \Delta_2(0)]B_\alpha^2\}^2 \\ - 4(B_\beta^2 - B_\alpha^2)[(\epsilon_2 - \epsilon_1)^2\Delta_4(1)\Delta_4(0)B_\beta^2 - (\epsilon_4 - \epsilon_3)^2\Delta_2(1)\Delta_2(0)B_\alpha^2]. \quad (4.24)$$

The imaginary parts of these eigenvalues determine the central frequency of each transition in the optical line, their real parts determine the corresponding linewidths. The association between the eigenvalues R_1, \dots, R_4 and the transitions in Fig. 2 depends on the relative magnitude of the model parameters.

To simplify the following discussion of the eigenvalues, we introduce the following approximations:

$$\Delta_4(1) = \Delta_2(1) = \Delta(1), \quad (4.25)$$

$$\Delta_4(0) = \Delta_2(0) = \Delta(0), \quad (4.26)$$

$$(\epsilon_4 - \epsilon_3), (\epsilon_2 - \epsilon_1) \gg \Delta(1)B_{\alpha,\beta}^2, \Delta(0)B_{\alpha,\beta}^2. \quad (4.27)$$

Equations (4.25) and (4.26) imply that the density of the phonons which contribute to the transitions between the levels with energies ϵ_1 and ϵ_2 and between the levels with energies ϵ_3 and ϵ_4 is the same. The assumption in (4.27) is that the transition rates (A12)–(A14) between the levels ϵ_1 and ϵ_2 and between ϵ_3 and ϵ_4 , and thus the lifetime broadening is much smaller than the energy splitting between the levels. The latter approximation is consistent with the Born approximation used in the derivation of the equation of motion for the reduced density operator.

With (4.25) and (4.26) the expression (4.23) for B simplifies to

$$B = -(\epsilon_4 - \epsilon_3)^2 - (\epsilon_2 - \epsilon_1)^2 + 2i(\epsilon_4 - \epsilon_3)[\Delta(1) - \Delta(0)]B_\beta^2 - 2i(\epsilon_2 - \epsilon_1)[\Delta(1) - \Delta(0)]B_\alpha^2 + [\Delta(1) + \Delta(0)]^2(B_\alpha^2 + B_\beta^2)^2. \quad (4.28)$$

In the discussion of the eigenvalues we need \sqrt{C} , and the expansion of this expression using (4.27) reads

$$2\sqrt{C} = 2(\epsilon_4 - \epsilon_3)(\epsilon_2 - \epsilon_1) - 2i(\epsilon_2 - \epsilon_1)[\Delta(1) - \Delta(0)]B_\beta^2 + 2i(\epsilon_4 - \epsilon_3)[\Delta(1) - \Delta(0)]B_\alpha^2 + 4\frac{\epsilon_2 - \epsilon_1}{\epsilon_4 - \epsilon_3}\Delta(1)\Delta(0)B_\beta^2(B_\alpha^2 - B_\beta^2) \\ - 4\frac{\epsilon_4 - \epsilon_3}{\epsilon_2 - \epsilon_1}\Delta(1)\Delta(0)B_\alpha^2(B_\alpha^2 - B_\beta^2). \quad (4.29)$$

From these expressions we obtain

$$B \pm 2\sqrt{C} = -[(\epsilon_4 - \epsilon_3) \mp (\epsilon_2 - \epsilon_1)]^2 + 2i[(\epsilon_4 - \epsilon_3) \mp (\epsilon_2 - \epsilon_1)][\Delta(1) - \Delta(0)](B_\beta^2 \pm B_\alpha^2) \\ + [\Delta(1) + \Delta(0)]^2(B_\alpha^2 + B_\beta^2)^2 \pm 4\frac{\epsilon_2 - \epsilon_1}{\epsilon_4 - \epsilon_3}\Delta(1)\Delta(0)B_\beta^2(B_\alpha^2 - B_\beta^2) \mp 4\frac{\epsilon_4 - \epsilon_3}{\epsilon_2 - \epsilon_1}\Delta(1)\Delta(0)B_\alpha^2(B_\alpha^2 - B_\beta^2). \quad (4.30)$$

Using (4.27) again, we have

$$(B - 2\sqrt{C})^{1/2} \approx i(\epsilon_4 - \epsilon_3 + \epsilon_2 - \epsilon_1) - [\Delta(1) - \Delta(0)]B_\alpha^2 + [\Delta(1) - \Delta(0)]B_\beta^2. \quad (4.31)$$

We insert this result into (4.21), and obtain for the eigenvalues R_3 and R_4 ,

$$R_3 = -i(\epsilon_3 - \epsilon_2) - \Delta(1)B_\alpha^2 - \Delta(0)B_\beta^2, \quad (4.32)$$

$$R_4 = -i(\epsilon_4 - \epsilon_1) - \Delta(0)B_\alpha^2 - \Delta(1)B_\beta^2. \quad (4.33)$$

In deriving this result we have assumed $B_\alpha^2 < B_\beta^2$. If $B_\alpha^2 > B_\beta^2$, R_3 and R_4 interchange with one another.

The eigenvalue R_3 describes a line centered at $\epsilon_3 - \epsilon_2$ whose width is determined by the real part of R_3 . $\Delta(1)B_\alpha^2$ describes transitions from level 2 to level 1 with the emission of a phonon, and $\Delta(0)B_\beta^2$ gives a contribution to the

linewidth due to transitions from level 3 to level 4 with the absorption of a phonon. The central position of the transition described by R_4 is at $\epsilon_4 - \epsilon_1$, and its width is determined by transitions from level 1 to level 2 due to phonon absorption, and from level 4 to level 3 due to emission of a phonon. Both eigenvalues have a finite real part also for $T \rightarrow 0$ K arising from spontaneous phonon emission.

In order to evaluate R_1 and R_2 we have to differentiate between two cases. In the first case of small phonon transition rates (slow motion), we have

$$|(\epsilon_4 - \epsilon_2) - (\epsilon_3 - \epsilon_1)| \gg \Delta(0)B_{\alpha,\beta}^2, \Delta(1)B_{\alpha,\beta}^2, \quad (4.34)$$

and the evaluation of $(B + 2\sqrt{C})^{1/2}$ results in

$$(B + 2\sqrt{C})^{1/2} \approx i(\epsilon_4 - \epsilon_2 - \epsilon_3 + \epsilon_1) + [\Delta(1) - \Delta(0)](B_\alpha^2 + B_\beta^2). \quad (4.35)$$

The eigenvalues R_1 and R_2 finally become

$$R_1 = -i(\epsilon_3 - \epsilon_1) - \Delta(0)(B_\alpha^2 + B_\beta^2), \quad (4.36)$$

$$R_2 = -i(\epsilon_4 - \epsilon_2) - \Delta(1)(B_\alpha^2 + B_\beta^2). \quad (4.37)$$

The imaginary parts indicate lines centered at $\epsilon_3 - \epsilon_1$ and $\epsilon_4 - \epsilon_2$. The real part of R_1 disappears for $T \rightarrow 0$ K, whereas the one of R_2 remains finite.

In the second case of rapid phonon transitions (fast motion leading to motional narrowing),

$$|(\epsilon_4 - \epsilon_2) - (\epsilon_3 - \epsilon_1)| \ll \Delta(0)B_{\alpha,\beta}^2, \Delta(1)B_{\alpha,\beta}^2, \quad (4.38)$$

and we define

$$h_2 = [\Delta(1) + \Delta(0)]^2(B_\alpha^2 + B_\beta^2)^2 + 4 \frac{\epsilon_2 - \epsilon_1}{\epsilon_4 - \epsilon_3} \Delta(1)\Delta(0)B_\beta^2(B_\alpha^2 - B_\beta^2) - 4 \frac{\epsilon_4 - \epsilon_3}{\epsilon_2 - \epsilon_1} \Delta(1)\Delta(0)B_\alpha^2(B_\alpha^2 - B_\beta^2). \quad (4.39)$$

Again expanding $(B + 2\sqrt{C})^{1/2}$ using (4.38), we have

$$\begin{aligned} (B + 2\sqrt{C})^{1/2} &= (h_2)^{1/2} + i(\epsilon_4 - \epsilon_3 - \epsilon_2 + \epsilon_1) \frac{[\Delta(1) - \Delta(0)](B_\alpha^2 + B_\beta^2)}{(h_2)^{1/2}} - \frac{1}{2} \frac{(\epsilon_4 - \epsilon_3 - \epsilon_2 + \epsilon_1)^2}{(h_2)^{1/2}} \\ &\quad + \frac{1}{2} \frac{(\epsilon_4 - \epsilon_3 - \epsilon_2 + \epsilon_1)^2}{(h_2)^{1/2}} \frac{[\Delta(1) - \Delta(0)]^2(B_\alpha^2 + B_\beta^2)^2}{h_2}. \end{aligned} \quad (4.40)$$

Inserting into (4.20) we obtain, for the eigenvalues,

$$\begin{aligned} \left. \begin{matrix} R_1 \\ R_2 \end{matrix} \right\} &= -\frac{i}{2} \left[(\epsilon_4 - \epsilon_2 + \epsilon_3 - \epsilon_1) \mp (\epsilon_4 - \epsilon_2 - \epsilon_3 + \epsilon_1) \frac{[\Delta(1) - \Delta(0)](B_\alpha^2 + B_\beta^2)}{(h_2)^{1/2}} \right] - \frac{1}{2} [\Delta(1) + \Delta(0)](B_\alpha^2 + B_\beta^2) \pm \frac{1}{2} (h_2)^{1/2} \\ &\quad \mp \frac{1}{4} \frac{(\epsilon_4 - \epsilon_2 - \epsilon_3 + \epsilon_1)^2}{(h_2)^{1/2}} \left[1 - \frac{[\Delta(1) - \Delta(0)]^2(B_\alpha^2 + B_\beta^2)^2}{h_2} \right] \end{aligned} \quad (4.41)$$

A detailed investigation of h_2 shows that, for

$$(V_\alpha - V_\beta)^2 \ll E^2, V_\alpha^2, V_\beta^2, \Delta^2, \quad (4.42)$$

the first term in h_2 is much larger than the following ones. Under these conditions the real parts of the eigenvalues are

$$\text{Re}(R_2) = -[\Delta(1) + \Delta(0)](B_\alpha^2 + B_\beta^2), \quad (4.43)$$

$$\text{Re}(R_1) = -\frac{\Delta(1)\Delta(0)}{\Delta(1) + \Delta(0)} W^2 \frac{(N_\beta - N_\alpha)^2}{(N_\alpha N_\beta)^{3/2}} - \frac{\Delta(1)\Delta(0)}{[\Delta(1) + \Delta(0)]^3} \frac{1}{W^2} N_\alpha N_\beta \frac{(N_\beta - N_\alpha)^2}{(N_\beta + N_\alpha)[(N_\beta)^{1/2} + (N_\alpha)^{1/2}]^2}, \quad (4.44)$$

with N_α given by

$$N_\alpha = E^2 - 4V_\alpha \Delta + 4V_\alpha^2. \quad (4.45)$$

N_β is obtained by replacing V_α in (4.45) by V_β . Finally, we specialize (4.44) to the case

$$E, \Delta \gg V_\alpha, V_\beta. \quad (4.46)$$

Then $\text{Re}(R_1)$ is given by

$$\text{Re}(R_1) = -\frac{\Delta(1)\Delta(0)}{\Delta(1) + \Delta(0)} 16 \frac{W^2 \Delta^2 (V_\alpha - V_\beta)^2}{E^6} - \frac{\Delta(1)\Delta(0)}{[\Delta(1) + \Delta(0)]^3} 2 \frac{\Delta^2 (V_\alpha - V_\beta)^2}{W^2}. \quad (4.47)$$

According to (4.41) in the case of motional narrowing, we have two imaginary parts which are slightly shifted away from the average value $\frac{1}{2}[(\epsilon_4 - \epsilon_2) + (\epsilon_3 - \epsilon_1)]$ to lower and higher frequencies, respectively. The real part of R_2 is increasing linearly (for high temperatures) with increasing temperature, which is obvious from comparison with the definition of $\Delta(0)$ and $\Delta(1)$ according to (4.25), (4.26), (A8)–(A11), and (3.8), and indicates a contribution to the optical line which broadens with increasing temperature. The real part of R_1 consists of two contributions, the first of which increases with increasing temperature, whereas the second decreases and describes a motional narrowing on account of the phonon-induced scattering between the energy levels ϵ_1 and ϵ_2 and between ϵ_3 and ϵ_4 . The first contribution to $\text{Re}(R_1)$ has been obtained recently^{31–33} and will be discussed in more detail in the following section.

V. AVERAGING OVER TLS'S

In the preceding section we have calculated the eigenvalues of a system of equations of motion for the correlation functions which describe the optical line shape. These calculations have been carried out for fixed values of the parameters of the system. The TLS's which are assumed to be characteristic for the glass, have, however, a broad distribution of system parameters. In the model of Anderson, Halperin, and Varma,²⁵ and of Phillips,²⁶ it is essential that the distribution function of the energy asymmetry is constant between zero and a maximum value Δ_{max} and decays rather rapidly outside of this range. The

tunneling matrix element W through the potential barrier of the double-well potential is given by

$$W = \omega_0 e^{-\lambda}, \quad (5.1)$$

where λ describes the overlap between the wave functions in the two minima of the potential. It is assumed^{25,26} that the distribution function is also constant in a range λ_{min} to λ_{max} . ω_0 is an attempt frequency of the TLS to tunnel through the barrier between the two minima, and is chosen to be of the order of the Debye frequency ω_D . We shall assume that we have also a distribution of ω_0 values. The interaction $V = V_\alpha - V_\beta$ between a TLS and the impurity, and the interaction $h = h^l - h^u$ between the vibrations of the matrix and a TLS, will also be different for various TLS's and must be described by a distribution function. We shall assume that the various distributions, except those for Δ and λ , are independent, which allows us to write

$$P(h, V, \omega_0, \Delta, \lambda) = P_h(h) P_V(V) P_{\omega_0}(\omega_0) P(\Delta, \lambda). \quad (5.2)$$

In the following discussion the detailed form of $P_h(h)$, $P_V(V)$, and $P_{\omega_0}(\omega_0)$ is not very important. We shall assume that they are normalized in the following way:

$$\int P_h(h) dh = 1, \quad (5.3)$$

$$\int P_V(V) dV = 1, \quad (5.4)$$

$$\int P_{\omega_0}(\omega_0) d\omega_0 = 1. \quad (5.5)$$

According to the model given in Refs. 25 and 26 the distribution function $P(\Delta, \lambda)$ is taken to be a constant

$$P(\Delta, \lambda) = \begin{cases} P \text{ independent of } \Delta \text{ and } \lambda \text{ for } 0 \leq \Delta \leq \Delta_{\text{max}}, \lambda_{\text{min}} \leq \lambda \leq \lambda_{\text{max}}, \\ 0 \text{ elsewhere.} \end{cases} \quad (5.6)$$

The normalization condition

$$\int_0^{\Delta_{\text{max}}} d\Delta \int_{\lambda_{\text{min}}}^{\lambda_{\text{max}}} d\lambda P(\Delta, \lambda) = 1 \quad (5.7)$$

results in

$$P = \frac{1}{\Delta_{\text{max}}(\lambda_{\text{max}} - \lambda_{\text{min}})}. \quad (5.8)$$

The average value of a function $\Delta\omega(h, V, \omega_0, \Delta, \lambda)$ is given by

$$\Delta\omega = \int dh \int dV \int d\omega'_0 \int d\Delta \int d\lambda \Delta\omega(h, V, \omega'_0, \Delta, \lambda) \times P(h, V, \omega'_0, \Delta, \lambda). \quad (5.9)$$

Transforming to new variables E , W , and ω_0 ,

$$E = \left[\Delta^2 + \omega_0'^2 e^{-2\lambda} \right]^{1/2}, \quad (5.10)$$

$$W = \omega_0' e^{-\lambda}, \quad (5.11)$$

$$\omega_0 = \omega_0', \quad (5.12)$$

we have

$$d\omega_0' d\Delta d\lambda = \frac{1}{W} \frac{E}{(E^2 - W^2)^{1/2}} d\omega_0 dW dE. \quad (5.13)$$

The average value now becomes

$$\langle \Delta\omega \rangle_{\text{av}} = \int dh \int dV \int d\omega_0 \int dE \int dW \Delta\omega(h, V, \omega_0, E, W) P_h(h) P_V(V) P_{\omega_0}(\omega_0) \frac{1}{\Delta_{\text{max}}(\lambda_{\text{max}} - \lambda_{\text{min}})} \frac{E}{W(E^2 - W^2)^{1/2}}. \quad (5.14)$$

From this expression we see that the distribution function in the new variables E and W is peaked at $E = W$. In the following we shall evaluate the first term^{31–33} of the linewidth (4.47), and use, for $\Delta\omega$ in (5.14),

$$\Delta\omega = 16W^2 \Delta^2 \frac{V^2}{E^6} \frac{\Delta(0)\Delta(1)}{\Delta(0) + \Delta(1)}. \quad (5.15)$$

Here we have used the abbreviation $(V_\alpha - V_\beta)^2 = V^2$. On

account of the approximations (4.25) and (4.26) and inserting (2.36) from (A8)–(A11), we have ($m=0,1$)

$$\Delta(m) = \sum_{qs} \pi \delta(\omega_{qs} - E) [n(\omega_{qs}) + m] \frac{h_{-qs}^l - h_{-qs}^u}{2\sqrt{N}} \frac{h_{qs}^l - h_{qs}^u}{2\sqrt{N}}. \quad (5.16)$$

In the following two subsections, (5.14) will be evaluated for interaction with acoustic and optical phonons separately.

A. Averaged linewidth for interaction with acoustic phonons

In this subsection we evaluate the averaged linewidth in the case of the interaction of the TLS's with acoustic phonons. The interaction matrix element may then be written in the following form:

$$h_{qs}^i = \delta_{sa} f^j (\omega_{qa} / 2Mc^2)^{1/2}, \quad j = l, u. \quad (5.17)$$

In writing this expression we assume that the TLS interacts only with a single acoustic branch. f^j is the deformation potential describing the interaction of the acoustic mode with the lower and upper states, respectively, in the TLS. c is the sound velocity of the mode and M is the mass of the unit cell. In the following it is convenient to use the abbreviation

$$f = f^l - f^u. \quad (5.18)$$

In the Debye approximation we have

$$\omega_{qa} = c |q| \quad (5.19)$$

and

$$\sum_{qs} \rightarrow \frac{V_0}{2\pi^2} \frac{1}{c^3} \int_0^{\omega_D} d\omega \omega^2, \quad (5.20)$$

where V_0 is the volume of the specimen. Equation (5.16) then becomes

$$\Delta(m) = \frac{1}{16\pi} \frac{1}{\rho c^5} f^2 E^3 [n(E) + m], \quad (5.21)$$

where we have introduced the mass density

$$\rho = NM/V_0. \quad (5.22)$$

Here N is the number of unit cells in the specimen. The evaluation of the last factor in (5.15) results in

$$\frac{\Delta(0)\Delta(1)}{\Delta(0) + \Delta(1)} = \frac{1}{32\pi} \frac{1}{\rho c^5} f^2 E^3 \frac{1}{\sinh(\beta E)}, \quad (5.23)$$

and the linewidth becomes

$$\Delta\omega = \frac{1}{2\pi} \frac{1}{\rho c^5} V^2 f^2 \frac{W^2(E^2 - W^2)}{E^3 \sinh(\beta E)}. \quad (5.24)$$

For the calculation of the averaged linewidth (5.14), we now assume that the attempt frequency ω_0 has a definite value ω_a which is smaller than the Debye frequency,

$$P_{\omega_0}(\omega_0) = \delta(\omega_0 - \omega_a), \quad \omega_a \leq \omega_D. \quad (5.25)$$

It is assumed^{26,26} that the maximum value of the energy asymmetry is larger than the Debye frequency,

$$\Delta_{\max} > \omega_D. \quad (5.26)$$

Therefore the maximum value of the energy splitting in the TLS, $E = (W^2 + \Delta^2)^{1/2}$, is larger than ω_D . However, on account of energy conservation in the interaction between TLS's and vibrations, which is expressed by the δ functions in (4.25) and (4.26), only TLS's with $E \leq \omega_D$ contribute to relaxation. Therefore the integration extends over the regime pictured in Fig. 3 instead of over the rectangle suggested by (5.6). Here we have introduced

$$W_1 = \omega_a e^{-\lambda_{\max}}, \quad W_2 = \omega_a e^{-\lambda_{\min}}, \quad (5.27)$$

which shows that W_1 and W_2 are smaller than ω_D , and

$$\Delta_1 = (\omega_D^2 - W_1^2)^{1/2}, \quad \Delta_2 = (\omega_D^2 - W_2^2)^{1/2}, \quad (5.28)$$

As mentioned in connection with (5.13), we use W and E as integration variables. The regime of integration in these variables is pictured in Fig. 4. For the evaluation of these integrals it is useful to introduce variables which are normalized to the Debye temperature and frequency, respectively,

$$y = \frac{E}{\omega_D}, \quad x = \frac{W}{\omega_D}, \quad (5.29a)$$

$$r = \omega_a / \omega_D, \quad \beta\omega_D = \omega_D / kT = \frac{1}{T_r}. \quad (5.29b)$$

Using (5.9) and (5.24), we then arrive at

$$\begin{aligned} \langle \Delta\omega \rangle_{av} = & \langle f^2 \rangle \langle V^2 \rangle \frac{1}{2\pi\rho c^5} \frac{\omega_D^2}{\Delta_{\max}(\lambda_{\max} - \lambda_{\min})} \\ & \times \left[\int_{x_1}^{x_2} dy \int_{x_1}^y dx + \int_{x_2}^1 dy \int_{x_1}^{x_2} dx \right] \\ & \times \frac{x(y^2 - x^2)^{1/2}}{y^2 \sinh(y/T_r)}. \end{aligned} \quad (5.30)$$

$\langle f^2 \rangle$ and $\langle V^2 \rangle$ are averages of interactions of the TLS's with vibrations and the ion. x_1 and x_2 are defined by

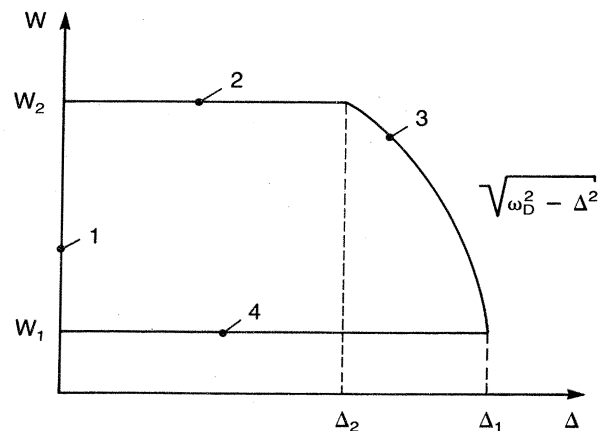


FIG. 3. Integration regime of the variables Δ and W for the evaluation of (5.14) in the case of acoustic phonons.

$$\begin{aligned} x_1 &= W_1/\omega_D = r e^{-\lambda_{\max}}, \\ x_2 &= W_2/\omega_D = r e^{-\lambda_{\min}}. \end{aligned} \quad (5.31)$$

Carrying out the x integration, we obtain

$$\begin{aligned} \langle \Delta\omega \rangle_{\text{av}} &= \langle f^2 \rangle \langle V^2 \rangle \frac{1}{2\pi\rho c^5} \frac{\omega_D^2}{\Delta_{\max}(\lambda_{\max} - \lambda_{\min})} \\ &\times \frac{2}{3} F_a(r, \lambda_{\min}, \lambda_{\max}, T_r), \end{aligned} \quad (5.32)$$

where

$$F_a = \frac{1}{2} \left[\int_{x_1}^{x_2} dy \frac{1}{y^2 \sinh(y/T_r)} (y^2 - x_1^2)^{3/2} + \int_{x_2}^1 dy \frac{1}{y^2 \sinh(y/T_r)} [(y^2 - x_1^2)^{3/2} - (y^2 - x_2^2)^{3/2}] \right]. \quad (5.33)$$

For high temperatures T_r , we may replace $\sinh(y/T_r)$ by its argument. Equation (5.33) then immediately shows that F_a is proportional to T_r and we recover the linear temperature dependence of the Lyo-Orbach²⁹ result. In the first integral this approximation is valid for $T_r \gg 10^{-2}$ if we assume $\lambda_{\min} = 5$, as is generally accepted.²⁵ In the second integral this approximation requires $T_r \gg 1$, and therefore we would expect the linear temperature dependence to be valid only above the Debye temperature. However, on account of the difference of the roots in the second integral, the integrand decays to zero rather rapidly and does not contribute to the integral near the upper limit. This has been shown in detail in a recent publication.³² The consequence of this partial compensation of the integrand is that the linewidth depends linearly on temperature not only above, but also below, the Debye temperature.

As is obvious from Fig. 1 of Ref. 32, for very low temperatures, the integrand decays rather rapidly on account of the hyperbolic sine function in the denominator. Therefore, if λ_{\min} is not too large, and thus x_2 is not too small, the second integral does not contribute to F_a . In the first integral we may replace the lower and upper limits by 0 and ∞ , respectively. If we neglect x_1 in the root of the first integral from dimensional considerations similar to those made in Ref. 31, we arrive at a quadratic increase of the linewidth with temperature, which, however, is valid only for low temperatures.

In the numerical evaluation of the temperature-dependent part F_a of the linewidth, we have assumed $r = 1$, i.e., $\omega_a = \omega_D$, and $\lambda_{\max} = 10$. The result is nearly independent of λ_{\max} for $\lambda_{\max} > 10$ and is shown in Fig. 5 for $\lambda_{\min} = 1, 3$, and 5 as a function of the reduced temperature. The curves show that the linewidth depends linearly on temperature also well below the Debye temperature. This is most clearly seen from the inset, which represents the range $0 < T_r < 0.01$ for $\lambda_{\min} = 5$. Another interesting

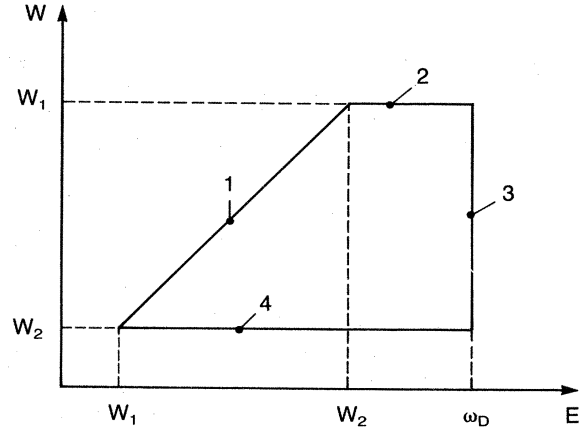


FIG. 4. Integration regime for the variables E and W resulting in (5.30).

result of the numerical evaluation is the strong dependence of F_a and thus of the dephasing time on the value of λ_{\min} . The physical reason for this increase in the dephasing rate is that, with decreasing λ , the interaction and therefore the splitting between the two energy levels of the TLS is increased. The density of acoustical phonons with this higher energy, however, increases quadratically within the Debye model, and thus gives rise to faster dephasing.

Comparing these results with the experimental temperature dependence of Hegarty and Yen,⁸ it is obvious that the model can explain only the very-low-temperature part

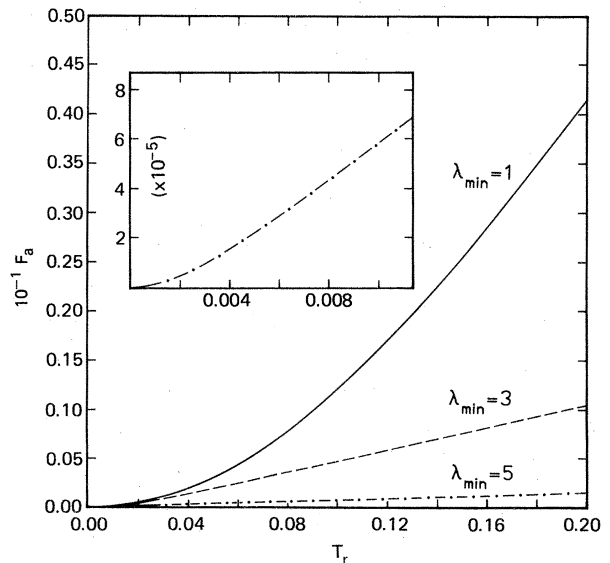


FIG. 5. F_a determining the temperature dependence of the linewidth for $\lambda_{\max} = 10$, and $\lambda_{\min} = 1, 3$, and 5. The inset shows F_a in the case of $\lambda_{\min} = 5$ for small values of T_r or an enlarged scale.

of the experimental curve. For higher temperatures other dephasing mechanisms, such as Raman processes and a direct coupling of the impurity to phonons, should be taken into account.

B. Averaged linewidth for coupling to optical phonons

A large number of experimental investigations of the temperature dependence of the linewidth of impurities in glasses has been carried out using organic matrices. In these materials in addition to the acoustic vibrations, optical and vibrational modes play an important role. For that reason, in this section we investigate the influence of these vibrations on the temperature dependence of impurity dephasing. As in the preceding section, the vibrations are coupled to the TLS, in contrast to the recent investigations of Jackson and Silbey³⁶ in which the librational modes are directly also coupled to the impurity.

The coupling matrix element between TLS's and phonons now becomes

$$h_{qs}^j = (\omega_s / \omega_D)^p g^j, \quad j = l, u \quad (5.34)$$

where $p = \frac{1}{2}$ (Ref. 44) or 1 .⁴⁵ We introduce the abbreviation

$$g = g^l - g^u, \quad (5.35)$$

and neglect the dispersion

$$\omega_{qs} \approx \omega_s. \quad (5.36)$$

Using $\sum_q 1 = N$ from (5.16), we obtain

$$\Delta(m) = \pi \sigma(E) [n(E) + m]^{\frac{1}{4}} (E / \omega_D)^{2p} g^2, \quad (5.37)$$

where the density of optical phonon models $\sigma(E)$ is given by

$$\sigma(E) = \sum_s \delta(\omega_s - E). \quad (5.38)$$

The temperature-dependent factor in (5.15) is given by

$$\frac{\Delta(0)\Delta(1)}{\Delta(0) + \Delta(1)} = \pi \sigma(E) \frac{1}{8} \left[\frac{E}{\omega_D} \right]^{2p} g^2 \frac{1}{\sinh(\beta E)}, \quad (5.39)$$

and (5.15) becomes

$$\langle \Delta \omega \rangle_{av} = \frac{2\pi \langle g^2 \rangle \langle V^2 \rangle}{\omega_D^2} \frac{1}{\Delta_{\max}(\lambda_{\max} - \lambda_{\min})} \left[\int_{y_{\min}}^{x_2} dy \int_{x_1}^y dx + \int_{x_2}^{y_1} dy + \int_{y_1}^{y_2} dy \int_{x_1}^{x_2} dx \int_{(y^2 - \Delta_r^2)^{1/2}}^{x_2} dx \right] \\ \times \frac{\sigma(y)}{\sinh(y/T_r)} \frac{x(y^2 - x^2)^{1/2}}{y^{5-2p}}. \quad (5.43)$$

Performing the x integration, we obtain, for the averaged linewidth, the following result:

$$\langle \Delta \omega \rangle_{av} = \frac{2\pi \langle g^2 \rangle \langle V^2 \rangle}{\omega_D^2} \frac{\sigma_y}{\Delta_{\max}(\lambda_{\max} - \lambda_{\min})} {}_3F_0(r, \lambda_{\min}, \lambda_{\max}, \Delta_r, y_{\min}, T_r), \quad (5.44)$$

with

$$F_0 = \frac{1}{2} \left[\int_{y_{\min}}^{x_2} dy \frac{1}{\sinh(y/T_r)} \frac{1}{y^{5-2p}} (y^2 - x_1^2)^{3/2} + \int_{x_2}^{y_1} dy \frac{1}{\sinh(y/T_r)} \frac{1}{y^{5-2p}} [(y^2 - x_r^2)^{3/2} - (y^2 - x_2^2)^{3/2}] \right. \\ \left. + \int_{y_1}^{y_2} dy \frac{1}{\sinh(y/T_r)} \frac{1}{y^{5-2p}} [\Delta_r^3 - (y^2 - x_2^2)^{3/2}] \right]. \quad (5.45)$$

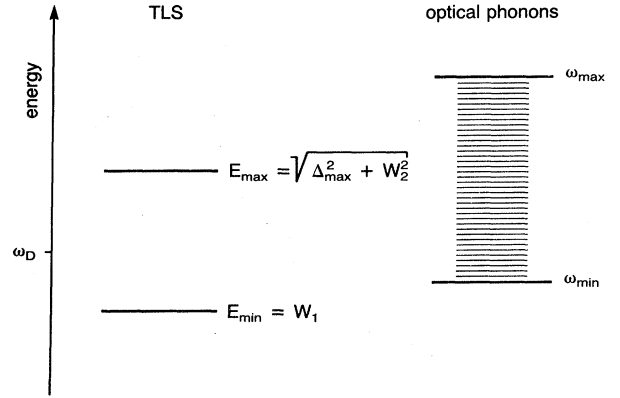


FIG. 6. Model for the density of optical modes.

$$\Delta \omega = 2\pi V^2 g^2 \sigma(E) \frac{W^2(E^2 - W^2)}{E^6} \frac{1}{\sinh(\beta E)} \left[\frac{E}{\omega_D} \right]^{2p}. \quad (5.40)$$

In order to carry out the averaging in (5.14) we have to specify the parameters in our model. In Fig. 6 the distribution of the energy splitting in the TLS's and the frequencies of the optical modes is presented. It is assumed that the energy splitting in the TLS's extends from some minimum value $E_{\min} = W_1$ below the Debye frequency to some minimum value $E_{\max} = (\Delta_{\max}^2 + W_2^2)^{1/2}$ above the Debye frequency. With respect to the density of optical modes, we assume that it is constant between a minimum value ω_{\min} below E_{\max} and a maximum value ω_{\max} above F_{\max} . Taking into account the energy conservation in the interaction process between TLS's and vibrations, we obtain the integration regime in Fig. 7 instead of the rectangle given in (5.6). Transformation to variables W and E gives the regime in Fig. 8. For the numerical evaluation of the integral (5.14), we introduce reduced variables as in (5.29), and in addition

$$\Delta_r = \Delta / \omega_D, \quad (5.41)$$

$$y_1 = (\Delta_r^2 + x_1^2)^{1/2}, \quad y_2 = (\Delta_r^2 + x_2^2)^{1/2}. \quad (5.42)$$

x_1 and x_2 are defined in (5.31). The integral now becomes

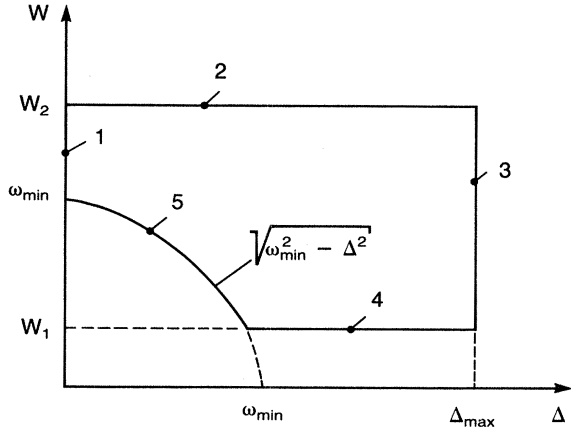


FIG. 7. Integration regime of the variables Δ and W for the evaluation of (5.14) in the case of optical phonons.

Here σ_y describes the constant density of librational modes. In the numerical evaluation we have assumed $p=1$, $r=1$, and $\Delta_r=2$, i.e., $\omega_a=\omega_D$, $\Delta_{\max}=2\omega_D$, and $\lambda_{\max}=10$. The temperature-dependent part of the linewidth F_0 is represented in Fig. 9 for $y_{\min}=0.5$ and in Fig. 10 for $y_{\min}=0.1$. The three curves in each figure represent F_0 for $\lambda_{\min}=3, 4$, and 5 , respectively. The inset gives the temperature dependence for λ_{\min} on an enlarged scale. From the figures it is clearly seen that the linewidth depends strongly on λ_{\min} . Comparison of Figs. 9 and 10 shows that the onset of the linewidth contribution from the optical phonons is strongly influenced by the value of y_{\min} . For larger values of y_{\min} , a smaller part of the TLS's contributes to the dephasing because of energy conservation, leading to slower dephasing and thus a smaller linewidth. Another interesting outcome of the numerical evaluation of the integrals is that as in the case of acoustic phonons the linear temperature dependence of the high-temperature approximation extends to rather low temperatures. The formal reason for this behavior is again the difference in terms in the integrand of (5.45). A numerical estimate³³ of the prefactor of the linewidth expression shows that the presence of low-frequency optical modes can influence the linewidth considerably.

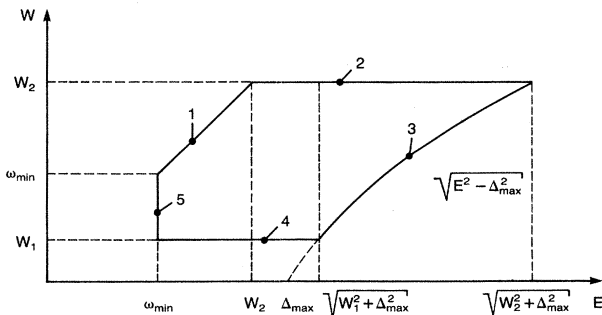


FIG. 8. Integration regime for the variables E and W resulting in (5.43).

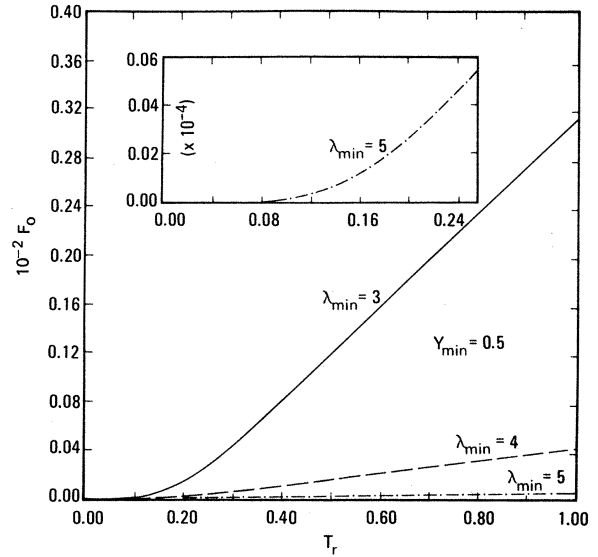


FIG. 9. F_0 determining the temperature dependence of the linewidth for the onset of the librational- and optical-mode frequencies $y_{\min}=0.5$ for $\lambda_{\min}=3, 4$, and 5 . The inset shows, on an enlarged scale, the nonlinear part of F_0 .

VI. CONCLUSIONS

In this paper we have presented the first treatment of optical dephasing of impurities in amorphous hosts using the density-operator approach. The density-matrix equation allows us to describe relaxation processes in the model used in the preceding sections, as well as to derive a coupled set of equations for the correlation functions describing the optical line shape.

We obtained, in Sec. IV, a full set of exact eigenvalues for the equivalent four-level problem describing the system part coupled to the bath, and give results in the weak

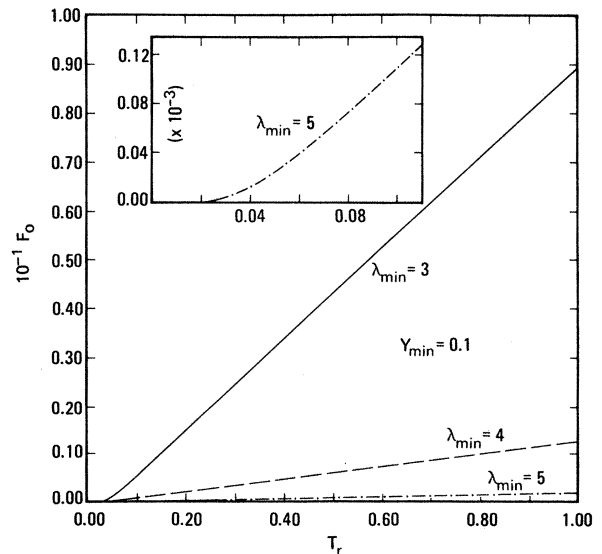


FIG. 10. Temperature dependence of the linewidth F_0 for $y_{\min}=0.1$. Note the crossover to a linear temperature dependence occurs at very low reduced temperature, $T_r \ll 1$.

coupling regime ($V_\alpha, V_\beta \ll E$). In the course of the full treatment for the various contributions to the optical linewidth, we have identified several different mechanisms for the temperature dependence: With increasing temperature we find lifetime broadening on the one hand and the Lyo-Orbach term and motional narrowing on the other.

We have introduced phonon-induced tunneling both via acoustic and optical vibrations (librations) with comparable contributions to the optical dephasing rate. The averaging over the various parameter ranges characterizing the TLS's has been performed and shows a strong dependence of the linewidth on the range limits.

We find that the crossover from quadratic to linear T dependence for acoustic-phonon-TLS coupling occurs at much lower temperature (by 2–3 orders of magnitude) than in the calculation of Lyo and Orbach. For coupling to optical modes, the crossover is from exponential to linear at temperatures determined by the lowest librational-mode frequency.

It is not possible to explain the Hegarty-Yen T dependence over the observed temperature range of several hundred degrees K. Another challenging problem is the absence of any break in the linewidth-versus-temperature curve. Additional theoretical and experimental work is needed to clarify presently open areas such as the direct coupling to phonons, higher-order scattering processes, and the influence of fractons.³⁷

ACKNOWLEDGMENTS

We wish to thank D. Haarer, R. Macfarlane, and S. Völker for discussions, and G. Castro for support and interest. One of us (H.M.) wishes to thank A. Schenzle for a careful reading of the manuscript. They also acknowledge the receipt of preprints from D. Huber, S. K. Lyo, R. Orbach, and R. Silbey.

APPENDIX A

Here we give the definition of the abbreviations introduced in Sec. III in connection with the derivation of the equation of motion for the density operator (3.9). We have

$$P_0 = \sum_{qs} P \frac{1}{\omega_{qs}} S_{-qs} D_{qs}, \quad (\text{A1})$$

$$P_1 = \sum_{qs} P \frac{1}{\omega_{qs}} D_{-qs} D_{qs}, \quad (\text{A2})$$

$$P_2(0) = \sum_{qs} [P_{21}^{qs}(0) - P_{12}^{qs}(1)] D_{-qs} D_{qs}, \quad (\text{A3})$$

$$P_2(1) = \sum_{qs} [P_{21}^{qs}(1) - P_{12}^{qs}(0)] D_{-qs} D_{qs}, \quad (\text{A4})$$

$$P_4(0) = \sum_{qs} [P_{43}^{qs}(0) - P_{34}^{qs}(1)] D_{-qs} D_{qs}, \quad (\text{A5})$$

$$P_4(1) = \sum_{qs} [P_{43}^{qs}(1) - P_{34}^{qs}(0)] D_{-qs} D_{qs}, \quad (\text{A6})$$

$$\Delta_0 = \sum_{qs} \pi \delta(\omega_{qs}) (2n_{qs} + 1) D_{-qs} D_{qs}, \quad (\text{A7})$$

$$\Delta_2(0) = \sum_{qs} [\delta_{21}^{qs}(0) + \delta_{12}^{qs}(1)] D_{-qs} D_{qs}, \quad (\text{A8})$$

$$\Delta_2(1) = \sum_{qs} [\delta_{21}^{qs}(1) + \delta_{12}^{qs}(0)] D_{-qs} D_{qs}, \quad (\text{A9})$$

$$\Delta_4(0) = \sum_{qs} [\delta_{43}^{qs}(0) + \delta_{34}^{qs}(1)] D_{-qs} D_{qs}, \quad (\text{A10})$$

$$\Delta_4(1) = \sum_{qs} [\delta_{43}^{qs}(1) + \delta_{34}^{qs}(0)] D_{-qs} D_{qs}, \quad (\text{A11})$$

$$W_{12} = 2\Delta_2(0) B_\alpha^2, \quad (\text{A12})$$

$$W_{21} = 2\Delta_2(1) B_\alpha^2, \quad (\text{A13})$$

$$W_{34} = 2\Delta_4(0) B_\beta^2, \quad (\text{A14})$$

$$W_{43} = 2\Delta_4(1) B_\beta^2, \quad (\text{A15})$$

$$\tilde{\epsilon}_1 = \epsilon_1 + 2P_0 A_\alpha - P_1 A_\alpha^2 + P_2(0) B_\alpha^2, \quad (\text{A16})$$

$$\tilde{\epsilon}_2 = \epsilon_2 - 2P_0 A_\alpha - P_1 A_\alpha^2 - P_2(1) B_\alpha^2, \quad (\text{A17})$$

$$\tilde{\epsilon}_3 = \epsilon_3 + 2P_0 A_\beta - P_1 A_\beta^2 + P_4(0) B_\beta^2, \quad (\text{A18})$$

$$\tilde{\epsilon}_4 = \epsilon_4 - 2P_0 A_\beta - P_1 A_\beta^2 - P_4(1) B_\beta^2, \quad (\text{A19})$$

APPENDIX B

Here we give an alternative, concise derivation of the connection between the equations of motion for the density-matrix and two-time correlation functions.

Expressing the density operator by the eigenstates (2.25) of the system Hamiltonian, we have

$$\rho = \sum_{i,j} \rho_{ij} |i\rangle \langle j|. \quad (\text{B1})$$

Its equation of motion is given by

$$\dot{\rho} = -i \sum_{ij} L |i\rangle \langle j| \rho_{ij}, \quad (\text{B2})$$

and can be written in the following way:

$$\dot{\rho} = -i \sum_{ij} \sum_{mn} C_{ij,mn} |m\rangle \langle n| \rho_{ij}, \quad (\text{B3})$$

$$\dot{\rho}_{mn} = - \sum_{ij} C_{ij,mn} \rho_{ij}. \quad (\text{B4})$$

In these expressions, $C_{ij,lm}$ is the tetrad corresponding to the superoperator L .

The two-time correlation functions in (4.8) are given by

$$K_{mn}(\tau) = \langle P^+ | e^{-iL\tau} | m \rangle \langle n | \rangle. \quad (\text{B5})$$

Differentiating with respect to τ and using (B2) and (B3), we have

$$\dot{K}_{mn}(\tau) = -i \langle P^+ | e^{-iL\tau} L | m \rangle \langle n | \rangle, \quad (\text{B6})$$

$$\dot{K}_{mn}(\tau) = -i \langle P^+ | e^{-iL\tau} \sum_{ij} C_{mn,ij} | i \rangle \langle j | \rangle. \quad (\text{B7})$$

Taking into account that $C_{mn,ij}$ are c numbers, and again using the definition of the correlation function, we find

$$\dot{K}_{mn}(\tau) = -i \sum_{ij} C_{mn,ij} K_{ij}(\tau), \quad (\text{B8})$$

showing that the matrices describing the time development of the density matrix and the correlation functions are transposed to each other.

- *On sabbatical leave from Abteilung für Theoretische Physik, Universität Ulm, 7900 Ulm, West Germany.
- ¹A. A. Gorokovskii, R. K. Kaarli, and L. A. Rebane, *Zh. Eksp. Teor. Fiz. Pis'ma Red* **20**, 474 (1974) [*JETP Lett.* **20**, 216 (1974)].
- ²B. M. Kharlamov, R. I. Personov, and L. A. Bykovskaya, *Opt. Commun.* **12**, 191 (1974).
- ³P. M. Selzer, D. L. Huber, D. S. Hamilton, W. M. Yen and M. J. Weber, *Phys. Rev. Lett.* **36**, 813 (1976).
- ⁴B. M. Kharlamov, L. A. Bykovskaya, and R. I. Personov, *Chem. Phys. Lett.* **50**, 407 (1977).
- ⁵P. Avouris, A. Campion, and M. A. El-Sayed, *J. Chem. Phys.* **67**, 3397 (1977).
- ⁶J. M. Hayes and G. J. Small, *Chem. Phys. Lett.* **54**, 435 (1978).
- ⁷J. M. Hayes and G. J. Small, *Chem. Phys.* **27**, 151 (1978).
- ⁸J. Hegarty and W. M. Yen, *Phys. Rev. Lett.* **43**, 1126 (1979).
- ⁹J. M. Hayes, R. P. Stout, and G. J. Small, *J. Chem. Phys.* **73**, 4129 (1980); **74**, 4266 (1981).
- ¹⁰J. Friedrich and D. Haarer, *Chem. Phys. Lett.* **74**, 504 (1980).
- ¹¹J. Friedrich, J. D. Swalen, and D. Haarer, *J. Chem. Phys.* **73**, 705 (1980).
- ¹²J. R. Morgan and M. A. El-Sayed, *Chem. Phys. Lett.* **84**, 213 (1981).
- ¹³E. Cuellar and G. Castro, *Chem. Phys.* **54**, 217 (1981).
- ¹⁴J. Friedrich, H. Scheer, B. Zickendraht-Wendelstadt, and D. Haarer, *J. Chem. Phys.* **74**, 2260 (1981).
- ¹⁵K. K. Rebane and A. A. Avarmaa, *J. Photochem.* **17**, 311 (1981).
- ¹⁶J. Friedrich and D. Haarer, *J. Chem. Phys.* **76**, 61 (1982); *Angew. Chem.* **96**, 96 (1984).
- ¹⁷J. Friedrich, H. Wolfrum, and D. Haarer, *J. Chem. Phys.* **77**, 2309 (1982).
- ¹⁸L. A. Rebane, A. A. Gorokovskii, and J. V. Kikas, *Appl. Phys. B* **29**, 235 (1982).
- ¹⁹H. P. H. Thijssen, A. I. M. Dicker, and S. Völker, *Chem. Phys. Lett.* **92**, 7 (1982).
- ²⁰H. P. H. Thijssen, R. van den Berg, and S. Völker, *Chem. Phys. Lett.* **97**, 295 (1983).
- ²¹R. Jankowiak and H. Bässler, *Chem. Phys. Lett.* **95**, 124 (1983); **95**, 310 (1983).
- ²²R. M. Macfarlane and R. M. Shelby, *Opt. Commun.* **45**, 46 (1983).
- ²³R. Shelby, *Opt. Lett.* **8**, 88 (1983).
- ²⁴*Proceedings of the Vth International Conference on Laser Spectroscopy*, edited by B. P. Stoicheff and T. Oka (Springer, Berlin, 1981).
- ²⁵P. W. Anderson, B. I. Halperin, and C. M. Varma, *Philos. Mag.* **25**, 1 (1972).
- ²⁶W. A. Phillips, *J. Low Temp. Physics* **7**, 351 (1972).
- ²⁷*Amorphous Solids. Low Temperature Properties*, Vol. 24 of *Topics in Current Physics*, edited by W. A. Phillips (Springer, Berlin, 1981).
- ²⁸T. L. Reinecke, *Solid State Commun.* **32**, 1103 (1979).
- ²⁹G. J. Small, in *Spectroscopy and Excitation Dynamics of Condensed Molecular Systems*, edited by V. M. Agranovich and R. M. Hochstrasser (North-Holland, Amsterdam, 1983).
- ³⁰I. Klafter and R. Silbey, *J. Chem. Phys.* **75**, 3973 (1981).
- ³¹S. K. Lyo and R. Orbach, *Phys. Rev. B* **22**, 4223 (1980).
- ³²P. Reineker and H. Morawitz, *Chem. Phys. Lett.* **86**, 359 (1982).
- ³³H. Morawitz and P. Reineker, *Solid State Commun.* **42**, 609 (1982).
- ³⁴S. K. Lyo, *Phys. Rev. Lett.* **48**, 688 (1982).
- ³⁵S. K. Lyo, *Theory of Dephasing of Impurities in Glasses, in Electronic Excitations and Interaction Processes in Organic Molecular Aggregates*, edited by P. Reineker, H. Haken, and H. C. Wolf, Vol. 49 of Springer Series in Solid State Sciences (Springer, Berlin, 1983).
- ³⁶B. Jackson and R. Silbey, *Chem. Phys. Lett.* **99**, 381 (1983).
- ³⁷R. Orbach, *Transport and Thermodynamics of Physical Systems with Fractal Geometry*, in Ref. 35.
- ³⁸S. Nakajima, *Prog. Theor. Phys.* **20**, 948 (1958).
- ³⁹R. Zwanzig, *J. Chem. Phys.* **33**, 1338 (1960).
- ⁴⁰F. Haake, in *Quantum Statistics in Optics and Solid State Physics*, Vol. 66 of *Springer Tracts in Modern Physics*, edited by G. Hoehler (Springer, Berlin, 1973).
- ⁴¹P. Reineker, in *Exciton Dynamics in Molecular Crystals and Aggregates*, Vol. 94 of Springer Tracts in Modern Physics, edited by G. Hoehler (Springer, Berlin, 1982).
- ⁴²H. Haken and W. Weidlich, *Z. Phys.* **205**, 96 (1967).
- ⁴³M. Lax, *Phys. Rev.* **157**, 213 (1967).
- ⁴⁴R. Silbey and R. Munn, *J. Chem. Phys.* **72**, 2763 (1980).
- ⁴⁵H. Sumi, *Solid State Commun.* **29**, 495 (1979).